Extended Frameworks Encapsulating Facial {MoO_3} Units: Syntheses and Structural Characterizations of $Ba_3(MoO_3)_3(H_2O)(AsO_4)_2$, $SrMoO_3HAsO_4 \cdot H_2O$, and $Sr(MoO_2AsO_4)_2$

Kuei-Fang Hsu and Sue-Lein Wang*

Department of Chemistry, National Tsing Hua University, Hsinchu, Taiwan 300

Received February 4, 1999. Revised Manuscript Received April 21, 1999

Three new alkaline earth metal molybdenum(VI) arsenates, $Ba_3(MoO_3)_3(H_2O)(AsO_4)_2$ (**1**), $SrMoO_3HAsO_4 \cdot H_2O$ (**2**), and $Sr(MoO_2AsO_4)_2$ (**3**), have been prepared and structurally characterized by single-crystal X-ray diffraction and thermogravimetric analysis. Crystal data: **1**, monoclinic, $P2_1/c$, $a = 10.1814(2)$ Å, $b = 17.5553(1)$ Å, $c = 17.0799(1)$ Å, $\beta = 90.349(1)°$, $V = 3052.75(7)$ Å^3, and $Z = 8$; **2**, monoclinic, $C2/c$, $a = 15.1927(11)$ Å, $b = 10.2590(8)$ Å, $c = 9.6550(7)$ Å, $\beta = 121.877(1)°$, $V = 1277.9(3)$ Å^3, and $Z = 8$; **3**, monoclinic, $P2_1/c$, $a = 6.5904(3)$ Å, $b = 6.8592(3)$ Å, $c = 10.4472(5)$ Å, $\beta = 92.106(2)°$, $V = 471.94(6)$ Å^3, and $Z = 2$. Crystal **1** adopts a novel open-framework structure which is composed of isolated MoO_6 and $Mo(H_2O)O_5$ octahedra linked by AsO_4 tetrahedra, resulting in intersecting tunnels where Ba^{2+} cations reside. Crystal **2** has a layer structure in which MoO_6 octahedra are corner-shared with $HAsO_4$ tetrahedra forming infinite sheets parallel to the (100) planes. The Sr^{2+} cations and water molecules are between the layers. Crystal **3** adopts a tunnel structure which is isotypic with the phosphates $A(MoO_2PO_4)_2$ (A = Ba, Pb). As a common feature, all of the MoO_6 octahedra possess three terminal O^{2-} ions in **1** and **2**. They are the first extended structures encapsulating facial {MoO_3} units. Thermal analysis and powder X-ray diffraction studies revealed that these units in **2** would progressively dissociate into cis {MoO_2} cores under heating, resulting in the structural transformation into **3**. In this paper, the syntheses, crystal structures, thermogravimetric studies, and structural relationship are presented.

Introduction

In the past decade the search for new open-framework materials has become a much interested and focused research area due to their potential applications as absorbents, ion exchangers, solid-state electrolytes, and catalysts in heterogeneous catalysis.[1−7] The microporous behavior was successfully extended into the phosphate and arsenate systems of titanium, vanadium, iron, cobalt, and molybdenum.[8−13] Syntheses of these materials usually involved organic templates for generating large cavities and were performed under mild hydrothermal conditions to avoid yielding dense phases. Recently, novel microporous compounds[6] of extremely low framework metal atom density (FD) were prepared by using inorganic countercations. By employing the Cs^+ cation as structure-directing reagent, we were able to obtain several interesting polyoxomolybdate anion structures[14,15] and the novel diarsenate, $Cs_2Mo_2O_5As_2O_7 \cdot H_2O$,[16] which is the most open metal arsenate framework ever reported.

Multidimensional extended structures in the Mo^{VI}/As^{V}/O system is very limited. The only examples include the layered $K_2MoO_2As_2O_7$[17] and $MoAs_2O_7$[18] and the tunneled $K_2(MoO_2)_3(As_2O_7)_2$[19] and $AMoO_2AsO_4$ (A = Li, Na, K).[20,21] To exploit more molybdenum (VI) arsenates characterized with open 3D framework, our investigation has been extended to divalent cations and more rigorous reaction conditions. Here, we report the first members in the alkaline earth metal/Mo^{VI}/As^{V}/O system: $Ba_3(MoO_3)_3(H_2O)(AsO_4)_2$ (**1**), $SrMoO_3HAsO_4 \cdot H_2O$

---

(1) Bu, X.; Feng, P.; Stucky, G. D. *Science* **1997**, *278*, 2080.
(2) Feng, P.; Bu, X.; Stucky, G. D. *Nature* **1997**, *388*, 735.
(3) Gier, T. E.; Bu, X.; Wang, S. L.; Stucky, G. D. *J. Am. Chem. Soc.* **1996**, *118*, 3039.
(4) Zubieta, J. *Comments Inorg. Chem.* **1994**, *16*, 153.
(5) Clearfield, A. *Chem. Rev.* **1988**, *88*, 125.
(6) Clearfield, A. *Comments Inorg. Chem.* **1990**, *10*, 89.
(7) Centi, G.; Trifiro, F.; Ebner, J. R.; Franchetti, V. M. *Chem. Rev.* **1988**, *88*, 55.
(8) Haushalter, R. C.; Mundi, L. A. *Chem. Mater.* **1992**, *4*, 31.
(9) Guesdon, A.; Borel, M. M.; Leclaire, A.; Grandin, A.; Raveau, B. *J. Solid State Chem.* **1994**, *111*, 315.
(10) Wang, S. L.; Lee, Y. H. *Inorg. Chem.* **1994**, *33*, 3845.
(11) Lii, K. H. *Inorg. Chem.* **1995**, *34*, 1700.
(12) Lii, K. H.; Huang, Y. F.; Zima, V.; Huang, C. Y.; Lin, H. M.; Jiang, Y. C.; Liao, F. L.; Wang, S. L.*Chem. Mater.* **1998**, *10*, 2599.
(13) Khan, M. I.; Meyer, L. M.; Haushalter, R. C.; Schwitzer, A. L.; Zubieta, J.; Dye, J. L. *Chem. Mater.* **1996**, *8*, 43.
(14) Hsu, K. F.; Wang, S. L. *Inorg. Chem.* **1997**, *36*, 3049.
(15) Wang, S. L.; Hsu, K. F.; Nieh, Y. P. *J. Chem. Soc., Dalton Trans.* **1994**, 1681.
(16) Hsu, K. F.; Wang, S. L. *Inorg. Chem.* **1998**, *37*, 3230.
(17) Zid, M. F.; Jouini, T. *Acta Crystallogr.* **1996**, *C52*, 1334.
(18) Hums, E.; Burzlaff, H.; Rothammel, W. *Acta Crystallogr.* **1993**, *C49*, 641.
(19) Zid, M. F.; Jouini, T. *Acta Crystallogr.* **1996**, *C52*, 2947.
(20) Zid, M. F.; Driss, A.; Jouini, T. *J. Solid State Chem.* **1997**, *133*, 386.
(21) Zid, M. F.; Jouini, T. *Acta Crystallogr.* **1996**, *C52*, 3.

10.1021/cm990072t CCC: $18.00

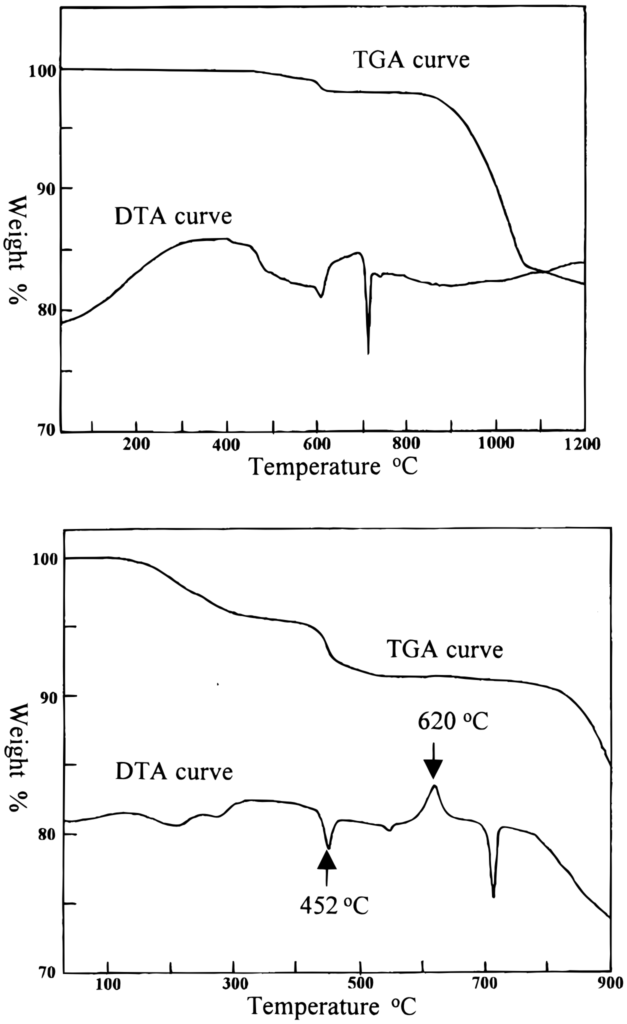

Figure 1. Thermogravimetric analysis of compound **1** (top) and compound **2** (bottom) in flowing N_2 at 10 °C min^{-1}.

Table 1. Crystallographic Data for 1, 2, and 3

	1	**2**	**3**
empirical formula	$H_2As_2Ba_3Mo_3O_{18}$	H_3AsMoO_8Sr	$AsMoO_6Sr_{0.5}$
fw	1139.7	389.5	310.7
space group	$P2_1/c$	$C2/c$	$P2_1/c$
a, Å	10.1814(2)	15.1927(11)	6.5904(3)
b, Å	17.5553(1)	10.2590(8)	6.8592(3)
c, Å	17.0799(1)	9.6550(7)	10.4472(5)
β, deg	90.349(1)	121.877(1)	92.106(2)
volume, Å^3	3052.75(7)	1277.9(3)	471.94(6)
Z	8	8	4
D_{cacl}, g cm^{-3}	4.951	4.409	4.372
μ, mm^{-1}	14.407	15.452	15.269
T, °C	23	23	23
λ, Å	0.71073	0.71073	0.71073
unique reflecns ($>3\sigma_I$)	6126	1302	844
$R(F_o)^a$	0.0392	0.0336	0.0418
$R_w(F_o)^b$	0.0450	0.0333	0.0473

[a] $R = \Sigma||F_o| - |F_c||/\Sigma|F_o|$. [b] $R_w = [\Sigma(|F_o| - |F_c|)^2/\Sigma w|F_o|^2]^{1/2}$, $w = [\sigma^2(F_o) + gF_o{}^2]^{-1}$, $g = 0.0005$ for **1**, 0.0 for **2**, and 0.0004 for **3**.

(**2**), and $Sr(MoO_2AsO_4)_2$ (**3**). Crystals of **1** were obtained from a hydrothermal reaction at 550 °C and 2200 atm. It adopts a open-framework structure having a low FD value comparable with that of very open faujasite.[22] The layered structure of **2** was prepared under mild hydrothermal conditions at 250 °C. Interestingly, both structures contain anti-Lipscomb facial {MoO_3} units[23–25] which have never been found in extended structures before. After dehydration, the layers in **2** fuse into the tunnel structure of **3**, accompanied by the dissociation of {MoO_3} into {MoO_2} cores under prolonged heating. In this paper, the syntheses, structures, thermogravimetric studies of **1** and **2**, and the structural relationship between **2** and **3** will be presented.

Experimental Section

Synthesis. Hydrothermal reactions were performed in gold ampules contained in a Leco Tem-Pres autoclave where pressure was provided by water. Chemicals of reagent grade were used as received. A mixture of $Ba(OH)_2{\cdot}8H_2O$ (0.0867 g, 0.275 mmol), MoO_2 (0.0352 g, 0.275 mmol), 3 M H_3AsO_4 (0.367 mL, 1.10 mmol), and H_2O (0.057 mL, 3.17 mmol) was heated at 550 °C and an estimated pressure of 2200 atm for 8 h followed by slow cooling (5 °C h^{-1}) to 250 °C and then cooled to room temperature by turning off the power of the furnace. The product was filtered off, washed with water, rinsed with ethanol, and dried in a desiccator. The final product,[26] which was nearly single phase, contained light-yellow columnar crystals of **1** and several colorless crystals of $BaHAsO_4$. Crystals of **2** were obtained under mild hydrothermal conditions: a mixture of $Sr(OH)_2{\cdot}8H_2O$ (0.0489 g, 0.184 mmol), MoO_3 (0.0264 g, 0.184 mmol), 3 M H_3AsO_4 (0.245 mL, 0.74 mmol), and water (0.062 mL, 3.44 mmol) was heated at 250 °C and ~40 atm for 48 h followed by slow cooling (5 °C h^{-1}) to room temperature. The product contained a pure phase of colorless tabular crystals of **2**. Compound **3** was prepared by a flux-growth method. A mixture of $SrCO_3$ (0.0295 g, 0.2 mmol), MoO_3 (0.0576 g, 0.4 mmol), and $NH_4H_2AsO_4$ (0.1272 g, 0.8 mmol) was ground in an agate mortar, placed in a 3 mL platinum crucible, and heated at 700 °C for 4 h, followed by a slow cooling (5 °C h^{-1}) to 400 °C and then quenched to room temperature. The melt was first dissolved in boiling water, and then a solid was obtained by suction filtration. The final product contained a pure phase of colorless equant crystals of **3**. X-ray powder patterns measured on the bulk samples compared well with the patterns simulated from the coordinates of single-crystal studies (see below). The A:Mo:As ratios of the compounds were also confirmed by the results of electron microprobe analyses.

Single-Crystal X-ray Diffraction Structure Analysis. Three crystals of dimensions 0.33 × 0.05 × 0.05 mm for **1**, 0.25 × 0.15 × 0.03 mm for **2**, and 0.23 × 0.14 × 0.12 mm for **3** were selected for indexing and intensity data collection. The diffraction measurements were performed on a Siemens Smart-CCD diffractometer system equipped with a normal focus, 3 kW sealed-tube X-ray source (λ = 0.710 73 Å). Intensity data were collected in 1271 frames with increasing ω (width of 0.3° per frame). Unit cell dimensions were determined by a least-squares fit of 6244 reflections for **1**, 3150 reflections for **2**, and 1608 reflections for **3**. The intensity data for the three crystals were corrected for *Lp* and absorption effects. The absorption correction was based on symmetry-equivalent reflections using the SADABS program.[27] On the basis of systematic absences and statistics of intensity distribution, the space group was determined to be $P2_1/c$ for **1**, $C2/c$ for **2**, and $P2_1/c$ for **3**. Direct methods were used to locate the alkaline earth metal, molybdenum, arsenic, and a few oxygen

---

(22) Meier, W. M.; Olson, D. H. *Atlas of Zeolite Structure Types*; Butterworth-Heinemann: Stoneham, MA, 1992.

(23) Lipscomb, W. N. *Inorg. Chem.* **1965**, *4*, 132.

(24) Pope, M. T. *Inorg. Chem.* **1972**, *11*, 1973.

(25) Pope, M. T.; Müller, A. *Polyoxometalates: From Platonic Solids to Anti-Retroviral Activity*; Kluwer: Dordrecht, 1994.

(26) The product would contain fine powders of compound **1** when the reaction was carried out using MoO_3 as the molybdenum source.

(27) Sheldrick, G. M. *SADABS*; Siemens Analytical X-ray Instrument Division: Madison, WI, 1995.

Table 2. Atomic Coordinates and Thermal Parameters (Å^2) for 1, 2, and 3

atom	x/a	y/b	z/c	U_{eq}[a]	atom	x/a	y/b	z/c	U_{eq}[a]
				1					
Ba(1)	−0.30315(5)	0.27011(3)	0.23930(3)	0.0181(1)	O(13)	0.3648(5)	0.2179(3)	0.4977(3)	0.018(2)
Ba(2)	0.20926(5)	0.08848(3)	0.50212(3)	0.0206(2)	O(14)	0.4274(5)	0.1620(3)	0.3577(3)	0.020(2)
Ba(3)	0.18704(5)	0.08146(3)	−0.00405(3)	0.0226(2)	O(15)	0.5528(5)	0.2941(3)	0.4068(3)	0.018(2)
Ba(4)	0.27681(6)	0.09044(3)	0.24348(3)	0.0253(2)	O(16)	0.2824(5)	0.2976(3)	0.3731(3)	0.016(2)
Ba(5)	0.30078(5)	0.40288(3)	0.24782(3)	0.0178(1)	O(17)	−0.1949(6)	0.1613(4)	0.1466(4)	0.025(2)
Ba(6)	0.78882(5)	0.23737(3)	0.48904(3)	0.0221(2)	O(18)	−0.0705(6)	0.0739(4)	0.0344(4)	0.028(2)
Mo(1)	−0.09113(7)	0.08301(4)	0.13517(4)	0.0166(2)	O(19)	−0.1912(6)	0.0058(4)	0.1560(4)	0.025(2)
Mo(2)	0.07818(6)	0.25142(4)	0.36909(4)	0.0142(2)	O_w[b](20)	−0.0557(7)	0.0859(4)	0.2675(4)	0.028(2)
Mo(3)	−0.08722(7)	0.42177(4)	0.12826(4)	0.0148(2)	O(21)	0.0585(6)	0.2648(4)	0.4700(4)	0.024(2)
Mo(4)	0.41277(7)	0.25151(4)	0.61025(4)	0.0148(2)	O(22)	0.1513(6)	0.1614(4)	0.3645(4)	0.025(2)
Mo(5)	0.59134(7)	0.07838(4)	0.36425(4)	0.0147(2)	O(23)	−0.0848(5)	0.2344(4)	0.3404(4)	0.022(2)
Mo(6)	0.57684(7)	0.41735(4)	0.38939(4)	0.0153(2)	O(24)	0.0741(6)	0.4351(4)	0.1622(4)	0.024(2)
As(1)	0.08436(8)	0.25643(5)	0.15884(5)	0.0138(2)	O(25)	−0.0650(7)	0.4133(4)	0.0263(4)	0.026(2)
As(2)	−0.09945(8)	0.41369(4)	0.33990(5)	0.0137(2)	O(26)	−0.1564(6)	0.5127(3)	0.1371(3)	0.021(2)
As(3)	0.58225(8)	0.08637(4)	0.57346(5)	0.0137(2)	O(27)	0.3458(6)	0.3424(3)	0.5979(4)	0.025(2)
As(4)	0.40888(8)	0.24411(5)	0.40639(5)	0.0135(2)	O(28)	0.5791(5)	0.2662(3)	0.5879(3)	0.019(2)
O(1)	0.0786(5)	0.1604(3)	0.1443(4)	0.022(2)	O(29)	0.4203(6)	0.2428(4)	0.7119(4)	0.025(2)
O(2)	0.1275(6)	0.2731(4)	0.2514(4)	0.030(2)	O(30)	0.7025(5)	0.0052(3)	0.3863(3)	0.019(2)
O(3)	−0.0589(5)	0.2973(3)	0.1318(4)	0.021(2)	O(31)	0.5303(6)	0.0472(3)	0.2741(3)	0.022(2)
O(4)	0.2106(5)	0.2965(3)	0.1118(3)	0.018(2)	O(32)	0.6976(6)	0.1528(4)	0.3420(4)	0.024(2)
O(5)	0.0470(5)	0.3742(3)	0.3626(4)	0.019(2)	O(33)	0.5644(6)	0.4019(3)	0.2893(4)	0.021(2)
O(6)	−0.1471(6)	0.3960(4)	0.2478(4)	0.024(2)	O(34)	0.4144(6)	0.4365(4)	0.4141(4)	0.026(2)
O(7)	−0.0876(5)	0.5088(3)	0.3535(4)	0.021(2)	O(35)	0.6469(6)	0.5073(4)	0.3977(4)	0.025(2)
O(8)	−0.2208(5)	0.3726(4)	0.3924(3)	0.019(2)	Ow(36)	0.6136(7)	0.4087(4)	0.5238(4)	0.027(2)
O(9)	0.7173(5)	0.1231(3)	0.6184(3)	0.018(2)	H(20A)	−0.0118	0.0468	0.2811	0.080
O(10)	0.5998(5)	0.1177(3)	0.4803(3)	0.018(2)	H(20B)	−0.0129	0.1258	0.2794	0.080
O(11)	0.4471(5)	0.1267(3)	0.6122(3)	0.019(2)	H(36A)	0.6947	0.4157	0.5335	0.080
O(12)	0.5769(5)	−0.0091(3)	0.5794(3)	0.020(2)	H(36B)	0.5687	0.4426	0.5470	0.080
				2					
Sr(1)	0.08005(4)	0.70728(5)	0.09718(6)	0.0193(2)	O(5)	0.3894(3)	0.3469(4)	0.6091(5)	0.022(2)
Mo(1)	0.34329(4)	0.42004(4)	0.71967(6)	0.0168(2)	O(6)	0.3667(4)	0.5831(4)	0.7149(6)	0.023(2)
As(1)	0.17772(4)	0.41083(5)	0.31125(7)	0.0150(3)	O(7)	0.4439(3)	0.3866(4)	0.9348(5)	0.023(2)
O(1)	0.1909(3)	0.4234(4)	0.4964(5)	0.017(2)	O_w(8)	−0.1006(4)	0.6842(4)	0.0972(5)	0.026(2)
O(2)	0.2216(3)	0.2740(4)	0.2741(5)	0.019(2)	H(4)	−0.00151	0.37991	0.10816	0.050
O(3)	0.2323(3)	0.5449(4)	0.2877(5)	0.020(2)	H(8A)	−0.13932	0.62435	0.03228	0.050
O_H[c](4)	0.0476(3)	0.4292(4)	0.1742(5)	0.020(2)	H(8B)	−0.11572	0.75725	0.03408	0.050
				3					
Sr(1)	0.5	0.0	0.5	0.0154(4)	O(3)	0.041(1)	−0.096(1)	1.136(1)	0.011(2)
Mo(1)	0.2447(1)	0.0486(1)	0.8361(1)	0.0075(3)	O(4)	0.253(1)	0.142(1)	1.301(1)	0.010(2)
As(1)	0.2577(1)	0.0358(2)	1.1564(1)	0.0081(3)	O(5)	0.282(1)	−0.177(1)	0.905(1)	0.014(2)
O(1)	0.279(1)	0.182(1)	1.029(1)	0.015(2)	O(6)	0.234(1)	−0.008(1)	0.679(1)	0.015(2)
O(2)	0.454(1)	−0.124(1)	1.162(1)	0.010(2)					

[a] U_{eq} is defined as one-third of the trace of the orthogonalized U_{ij} tensor. [b] The symbol O_w stands for water oxygen. [c] The symbol OH stands for hydroxo oxygen.

atoms with the remaining non-hydrogen atoms being found from successive difference maps. The results of bond-valence-sum calculations[28] were used to identify the hydroxo and water oxygen atoms respectively in **1** and **2**. The hydrogen atoms in **1** were calculated using a riding model. The hydrogen atoms in **2** were directly located from a Fourier difference map calculated at the final stage of structure refinements. The final cycle of refinement, including the atomic coordinates and anisotropic thermal parameters for all non-hydrogen atoms and fixed atomic coordinates and isotropic thermal parameters for the hydrogen atoms, converged at $R = 0.0392$ and $R_w = 0.0450$ for **1**, $R = 0.0336$ and $R_w = 0.0331$ for **2**, and $R = 0.0418$ and $R_w = 0.0473$ for **3**. Corrections for secondary extinction and anomalous dispersion were applied. Neutral-atom scattering factors for all atoms were taken from the standard sources. Calculations were performed on DEC VAX 4000/90 workstations using the SHELXTL-Plus programs.[29]

Thermal Analysis. Thermogravimetric analyses were performed on powder samples of **1** and **2** in flowing N_2 with a heating rate of 10 °C min^{-1}. The TG and DT curves are shown in Figure 1. Before 800 °C, the TG curve of **1** shows a weight loss of ca. 1.9% in the temperature range 450−630 °C, corresponding to the evolution of one coordinated water molecule. Beyond 800 °C the sharp fall in weight can be attributed to the evolution of O_2(g) and sublimation of As_2O_3.[14−16] The TG curve of **2** shows two steps of weight loss before decomposition. The first step occurring between 100 and ca. 350 °C corresponds to the lattice water evolution. The second step occurring in the ca. 350−620 °C range corresponds to the elimination of $^1/_2H_2O$ and $^1/_4O_2$(g). These two steps are not resolved well from each other, but the total observed weight loss (8.8%) is in good agreement with the calculated value (8.98%). The sharp fall in weight above 800 °C can be as well attributed to the evolution of O_2(g) and sublimation of As_2O_3 as occurred in **1**.

There is one exothermic peak appearing at ca. 620 °C in the DT curve of **2** without a counterpart in TG curve, indicating the possible emergence of a new phase from the thermal product. To identify this phase, two samples of **2** were separately heated at 550 °C and 680 °C. Powder X-ray diffraction patterns showed that the product of the thermal treatment obtained at 680 °C contained a predominant phase of **3**.

Results and Discussion

The crystallographic data for **1**, **2**, and **3** are listed in Table 1. Atomic coordinates and thermal parameters are in Table 2, and selected bond lengths and bond-valence

---

(28) Brown, I. D.; Altermann, D. *Acta Crystallogr.* **1985**, *B41*, 244.
(29) Sheldrick, G. M. *SHELXTL-Plus Crystallographic System*, Release 4.21; Siemens Analytical X-ray Instrument Division: Madison, WI, 1991.

Table 3. Selected Bond Lengths (Å) and Bond Valence Sums ($\sum s$) for 1, 2, and 3[a]

1							
Ba(1)−O(32)[a]	2.705(6)	Ba(1)−O(33)[a]	2.813(6)	Mo(2)−O(22)	1.748(6)	Mo(2)−O(2)	2.110(6)
Ba(1)−O(17)	2.719(6)	Ba(1)−O(29)[b]	2.860(6)	Mo(2)−O(23)	1.753(6)	Mo(2)−O(5)	2.180(6)
Ba(1)−O(6)	2.726(6)	Ba(1)−O(23)	2.876(6)	Mo(2)−O(21)	1.752(6)	Mo(2)−O(16)	2.232(5)
Ba(1)−O(9)[b]	2.797(6)	Ba(1)−O(28)[b]	2.913(6)	$\sum s$[Mo(2)−O] = 6.07			
$\sum s$[Ba(1)−O] = 2.02				Mo(3)−O(26)	1.751(6)	Mo(3)−O(9)[b]	2.147(6)
Ba(2)−O(30)[c]	2.669(6)	Ba(2)−O(26)[e]	2.775(6)	Mo(3)−O(24)	1.754(6)	Mo(3)−O(6)	2.182(6)
Ba(2)−O(22)	2.739(6)	Ba(2)−O(25)[d]	2.825(7)	Mo(3)−O(25)	1.763(6)	Mo(3)−O(3)	2.205(6)
Ba(2)−O(4)[d]	2.755(6)	Ba(2)−O(12)[c]	2.942(6)	$\sum s$[Mo(3)−O]= 5.96			
Ba(2)−O(13)	2.770(6)	Ba(2)−O(24)[d]	3.096(6)	Mo(4)−O(29)	1.745(6)	Mo(4)−O(13)	2.066(5)
$\sum s$[Ba(2)−O] = 2.01		Ba(2)−O(11)	3.130(6)	Mo(4)−O(27)	1.748(6)	Mo(4)−O(11)	2.219(6)
Ba(3)−O(18)	2.710(7)	Ba(3)−O(19)[h]	3.014(6)	Mo(4)−O(28)	1.757(5)	Mo(4)−O(4)[d]	2.225(5)
Ba(3)−O(27)[f]	2.719(6)	Ba(3)−O(18)[h]	3.018(7)	$\sum s$[Mo(4)−O] = 6.09			
Ba(3)−O(34)[f]	2.730(6)	Ba(3)−O(21)[f]	3.031(6)	Mo(5)−O(32)	1.739(6)	Mo(5)−O(10)	2.100(5)
Ba(3)−O(5)[f]	2.791(6)	Ba(3)−O(7)[e]	3.049(6)	Mo(5)−O(30)	1.751(6)	Mo(5)−O(14)	2.225(6)
Ba(3)−O(35)[g]	2.796(6)	Ba(3)−O(1)	3.098(6)	Mo(5)−O(31)	1.745(6)	Mo(5)−O(12)[c]	2.316(6)
$\sum s$[Ba(3)−O] = 2.08				$\sum s$[Mo(5)−O] = 6.00			
Ba(4)−O(22)	2.736(6)	Ba(4)−O(27)[f]	2.844(6)	Mo(6)−O(33)	1.735(6)	Mo(6)−O(15)	2.198(6)
Ba(4)−O(31)	2.738(6)	Ba(4)−O(1)	2.900(6)	Mo(6)−O(35)	1.738(6)	Mo(6)−O(8)[k]	2.205(5)
Ba(4)−O(26)[e]	2.749(6)	Ba(4)−O(7)[e]	2.911(6)	Mo(6)−O(34)	1.742(6)	Mo(6)−O$_w$(36)	2.329(6)
Ba(4)−O(14)	2.774(6)	Ba(4)−O(35)[g]	2.927(6)	$\sum s$[Mo(6)−O] = 6.00			
$\sum s$[Ba(4)−O] = 1.91				As(1)−O(1)	1.706(6)	As(1)−O(3)	1.688(6)
Ba(5)−O(19)[i]	2.689(6)	Ba(5)−O(16)	2.835(6)	As(1)−O(2)	1.664(6)	As(1)−O(4)	1.674(6)
Ba(5)−O(33)	2.772(6)	Ba(5)−O(2)	2.882(7)	$\sum s$[As(1)−O] = 5.02			
Ba(5)−O(24)	2.784(6)	Ba(5)−O(29)[f]	2.900(6)	As(2)−O(5)	1.687(5)	As(2)−O(7)	1.689(6)
Ba(5)−O(11)[f]	2.810(6)	Ba(5)−O(30)[j]	2.911(6)	As(2)−O(6)	1.672(6)	As(2)−O(8)	1.692(6)
$\sum s$[Ba(5)−O] = 2.02		Ba(5)−O(31)[j]	3.086(6)	$\sum s$[As(2)−O] = 4.99			
Ba(6)−O(28)	2.777(6)	Ba(6)−O(3)[l]	2.945(6)	As(3)−O(9)	1.698(6)	As(3)−O(11)	1.686(6)
Ba(6)−O(21)[k]	2.809(6)	Ba(6)−O(15)	2.949(5)	As(3)−O(10)	1.694(5)	As(3)−O(12)	1.679(6)
Ba(6)−O(10)	2.853(6)	Ba(6)−O(32)	3.058(6)	$\sum s$[As(3)−O] = 4.94			
Ba(6)−O(23)[k]	2.853(6)	Ba(6)−O(9)	3.075(6)	As(4)−O(13)	1.690(5)	As(4)−O(15)	1.708(5)
Ba(6)−O(8)[k]	2.893(6)	Ba(6)−O(25)[l]	3.099(6)	As(4)−O(14)	1.676(6)	As(4)−O(16)	1.689(5)
$\sum s$[Ba(6)−O] = 1.82				$\sum s$[As(4)−O] = 4.92			
Mo(1)−O(19)	1.734(6)	Mo(1)−O(1)	2.202(6)				
Mo(1)−O(17)	1.745(6)	Mo(1)−O(7)[e]	2.246(6)				
Mo(1)−O(18)	1.743(7)	Mo(1)−O$_w$(20)	2.287(6)				
$\sum s$[Mo(1)−O] = 5.91							
2							
Sr(1)−O(7)[m]	2.587(4)	Sr(1)−O(5)[o]	2.685(6)	As(1)−O(1)	1.695(5)	As(1)−O(3)	1.682(5)
Sr(1)−O(3)	2.648(4)	Sr(1)−O(1)[q]	2.704(5)	As(1)−O(2)	1.673(5)	As(1)−O(4)	1.712(4)
Sr(1)−O(6)[n]	2.649(4)	Sr(1)−O$_w$(8)	2.755(6)	$\sum s$[As(1)−O] = 4.92			
Sr(1)−O(2)[o]	2.671(5)	Sr(1)−O$_w$(8)[r]	2.808(6)	O(4)−H(4)	0.847	O$_w$(8)−H(8A)	0.852
Sr(1)−O(4)[p]	2.687(4)	Sr(1)−O(4)	3.053(4)	O$_w$(8)−H(8B)	0.916		
$\sum s$[Sr(1)−O] = 2.03							
Mo(1)−O(6)	1.716(4)	Mo(1)−O(3)[s]	2.139(6)				
Mo(1)−O(5)	1.727(6)	Mo(1)−O(1)	2.176(3)				
Mo(1)−O(7)	1.848(4)	Mo(1)−O(2)[s]	2.236(4)				
$\sum s$[Mo(1)−O] = 5.90							
3							
Sr(1)−O(6)	2.608(8)	Sr(1)−O(4)[v]	2.771(7)	Mo(1)−O(6)	1.686(8)	Mo(1)−O(2)[v]	2.052(7)
Sr(1)−O(6)[c]	2.608(8)	Sr(1)−O(5)[w]	2.801(7)	Mo(1)−O(5)	1.723(7)	Mo(1)−O(4)[f]	2.156(7)
Sr(1)−O(1)[t]	2.646(8)	Sr(1)−O(5)[x]	2.801(7)	Mo(1)−O(3)[y]	1.946(7)	Mo(1)−O(1)	2.218(8)
Sr(1)−O(1)[f]	2.646(8)	Sr(1)−O(2)[w]	3.110(7)	$\sum s$[Mo(1)−O] = 5.98			
Sr(1)−O(4)[u]	2.771(7)	Sr(1)−O(2)[x]	3.110(7)	As(1)−O(1)	1.676(8)	As(1)−O(3)	1.697(7)
$\sum s$[Sr(1)−O] = 1.81				As(1)−O(2)	1.692(7)	As(1)−O(4)	1.675(7)
				$\sum s$[As(1)−O] = 4.99			

[a] Symmetry codes: (a) $-1 + x, y, z$; (b) $-1 + x, {}^1/_2 - y, -{}^1/_2 + z$; (c) $1 - x, -y, 1 - z$; (d) $x, {}^1/_2 - y, {}^1/_2 + z$; (e) $-x, -{}^1/_2 + y, {}^1/_2 - z$; (f) $x, {}^1/_2 - y, -{}^1/_2 + z$; (g) $1 - x, -{}^1/_2 + y, {}^1/_2 - z$; (h) $-x, -y, -z$; (i) $-x, {}^1/_2 + y, {}^1/_2 - z$; (j) $1 - x, {}^1/_2 + y, {}^1/_2 - z$; (k) $1 + x, y, z$; (l) $1 + x, {}^1/_2 - y, {}^1/_2 + z$; (m) $-{}^1/_2 + x, {}^1/_2 + y, -1 + z$; (n) ${}^1/_2 - x, {}^3/_2 - y, 1 - z$; (o) ${}^1/_2 - x, {}^1/_2 + y, {}^1/_2 - z$; (p) $-x, 1 - y, -z$; (q) $x, 1 - y, -{}^1/_2 + z$; (r) $-x, y, {}^1/_2 - z$; (s) ${}^1/_2 - x, {}^1/_2 - y, 1 - z$; (t) $1 - x, -{}^1/_2 + y, {}^3/_2 - z$; (u) $x, y, -1 + z$; (v) $1 - x, -y, 2 - z$; (w) $1 - x, {}^1/_2 + y, {}^3/_2 - z$; (x) $x, -{}^1/_2 - y, -{}^1/_2 + z$; (y) $-x, -y , 2- z$.

sums are in Table 3. The Mo and As atoms are six- and four-coordinated, respectively. The coordination numbers of the Ba atoms range from 8 to 10 in **1** and that of the Sr atoms is 10 in both **2** and **3**. The determination was based on the maximum gap in the cation−oxygen distances ranked in increasing order and the maximum cation−oxygen distances.[30] As shown in Table 3, the bond-valence sums for atoms Mo, As, Ba, and Sr are all in good accordance with their formal oxidation states.

As depicted in Figure 2, the asymmetric unit of the structure **1** contains six octahedra of four MoO_6 and two $Mo(H_2O)O_5$ and four tetrahedra of AsO_4. Each MoO_6 octahedron connects to three tetrahedra, each $Mo(H_2O)O_5$ to two tetrahedra, and each tetrahedron to four octahedra. The connectivity results in a novel open framework with intersecting tunnels in the directions of [010] and [001]. The Ba cations are located at the intersection points of the two-way tunnels. Alternatively, structure **1** may be viewed as stacking of the porous sheets, shown in Figure 3, along [001] with

---

(30) *Tables of Interatomic Distances and Configuration in Molecules and Ions*; Chemical Society Special Publication No. 11; Chemical Society: London, 1958.

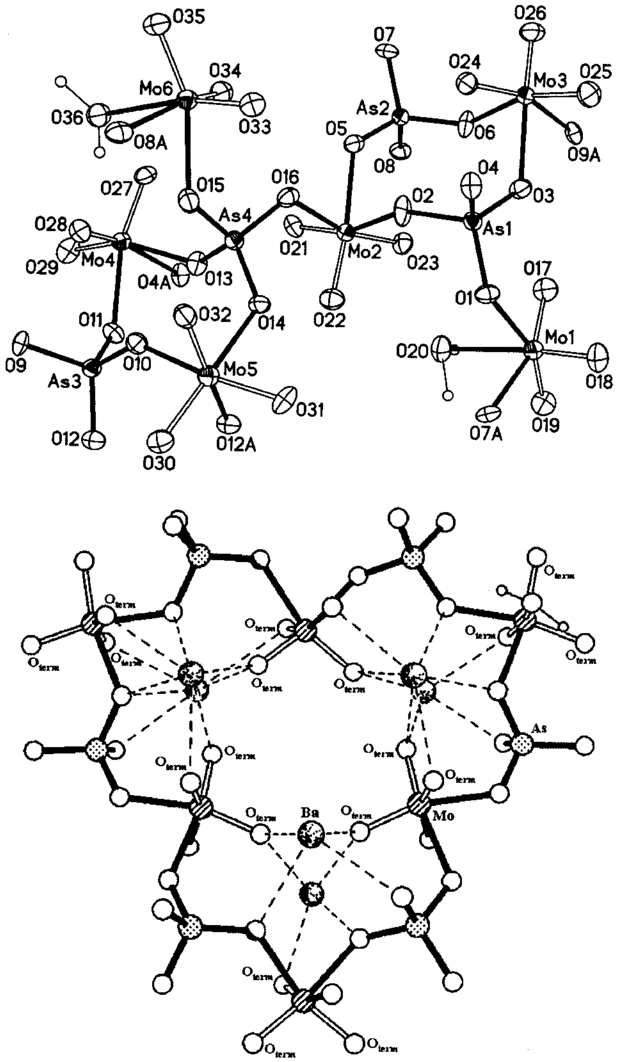

Figure 2. Ball and stick plots of structure **1**. (top) ORTEP drawing of the asymmetric unit. Open bonds are used to denote $Mo{=}O_{term}$ groups. Thermal ellipsoids are drawn at the 50% level. (bottom) Drawing of a 12-membered ring in the porous sheet (see text) showing the interactions between the framework oxygen atoms and barium cations. The O^{2-} ions belonging to the facial $\{MoO_3\}$ units are labeled as O_{term}. Note that each O_{term} makes two ionic bonds with Ba^{2+} cations. In the plot, striped circles are Mo atoms, dotted circles are As atoms, large open circles are O atoms, small open circles are H atoms, and stippled circles are Ba atoms. Dash lines represent Ba−O bonds.

adjacent sheets being related by 21 symmetry. Each sheet is composed of 12-membered rings with a diameter (minimum O···O distance less one O diameter of 2.8 Å) of ~7.8 Å. Large cavities result along the stacking directions. The empty interstitial space inside the structure is quite noticeable as its framework metal atom density (FD), 13.1 M atoms (M = Mo, As)/1000 Å^3, being comparable with that of the very open faujasite (FD = 12.7 M atoms/1000 Å^3, M = Si).[22]

One interesting feature of **1** is in that all octahedra in the framework contain facial $\{MoO_3\}$ units, which has never been found in extended structures before. According to the Lipscomb rule,[23] aggregation of MoO_6 octahedra with three terminal O^{2-} ions should be unstable because the strong trans effect generated from the three $Mo{=}O_{term}$ groups might result in the dissociation of facial $\{MoO_3\}$ units attached to the structure.

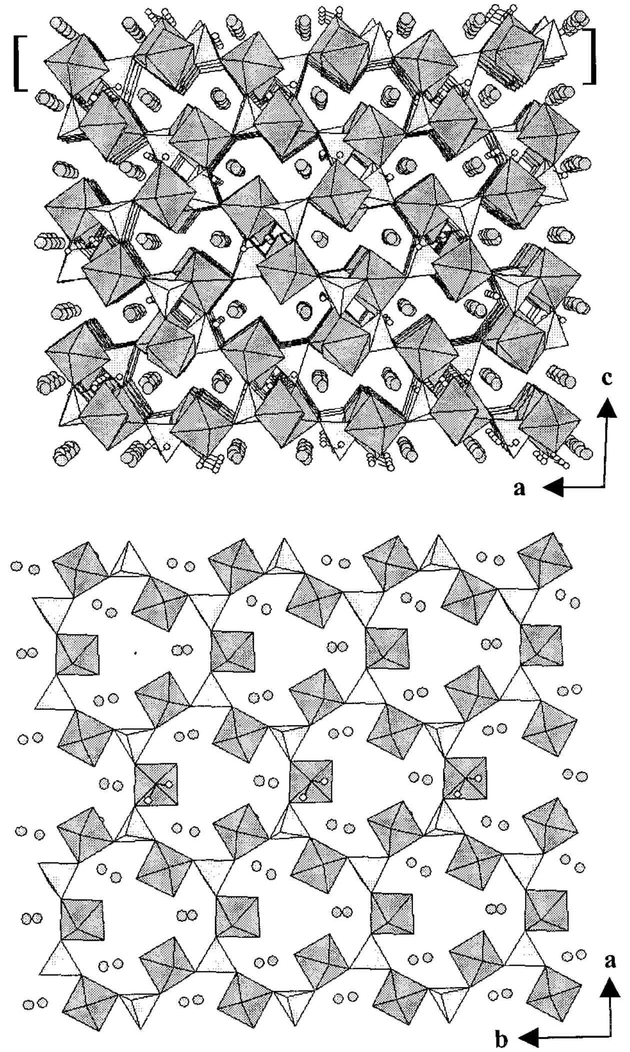

Figure 3. Polyhedral representations of structure **1**. (top) Projection down to the *b*-axis. The structure can be viewed as stacking of the polyhedral sheet (marked in a square bracket) along [001]. (bottom) Section of the porous sheet containing 12-membered rings with a diameter of ~7.8 Å. In these representations, the darker polyhedra are MoO_6 octahedra, the lighter ones are AsO_4 tetrahedra, large circles are Ba atoms, and small circles are H atoms.

Exceptions to the Lipscomb rule were limited to several polyalkoxomolybdate structures[31−34] in which the minority of electrophilic $\{MoO_3\}$ groups are stabilized by the basic surface oxygen bonded to the majority of reduced Mo(V) atoms. In justification of the stability of $\{MoO_3\}$ groups in **1**, barium cations may play an important role. It is noticed that each of the O_{term} atoms receives an average bond valence of 1.54 valence units (vu) from the anionic framework, far away from saturation. But in the presence of countercations, each O_{term} atom has two short contacts with Ba^{2+} cations (Figure 2) and receives an additional bond valence of ~0.45 vu. In total, the bond-valence sums of all terminal O atoms are saturated. Accordingly, the facial $\{MoO_3\}$ units are well stabilized in structure **1**.

---

(31) Ma, L.; Liu, S.; Zubieta, J. *Inorg. Chem.* **1989**, *28*, 175.

(32) Khan, M. I.; Müller, A.; Dillinger, S.; Bögge, H.; Chen, Q.; Zubieta, J. *Angew. Chem., Int. Ed. Engl.* **1993**, *32*, 1780.

(33) Khan, M. I.; Chen, Q.; Salta, J.; O'connor, C. J.; Zubieta, J. *Inorg. Chem.* **1996**, *35*, 1880.

(34) Müller, A.; Krickemeyer, E.; Dillinger, S.; Meyer, J.; Bögge, H.; Stammler, A. *Angew. Chem., Int. Ed. Engl.* **1996**, *35*, 171.

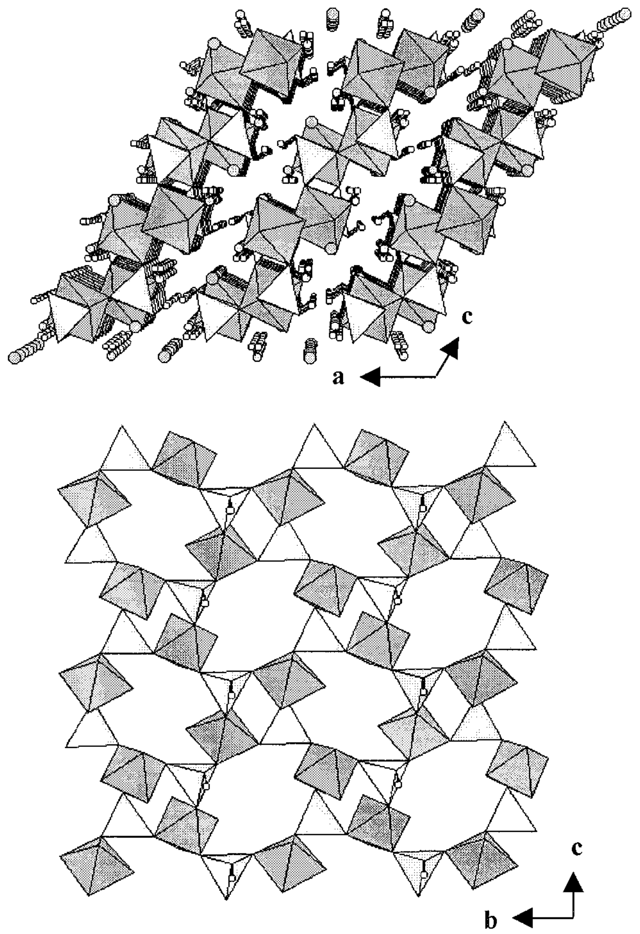

Figure 4. Structural plots of structure **2**. (a, top) A perspective view along the [010] direction. (b, bottom) Section of a layer showing the eight- and four-membered rings.

It is also interesting to note that, besides the three terminal O^{2-} ions, one-third of the octahedra, $Mo(H_2O)O_5$, carry a water molecule as the fourth unshared vertice, namely, the $\{MoO_4H_2\}$ core, a rare species in molybdenum chemistry. Coordination polyhedra with four unshared vertexes have been inclusively $Mo^{VI}O_4$ tetrahedron in the literature.[35−37] TG analysis shows that the coordinated water moleculeevolves at a temperature up to 450 °C (see Figure 1), which is exceptionally high for coordinated H_2O.[38−40] The strong resistance of the $\{MoO_4H_2\}$ core to dehydration makes compound **1** the most thermally stable molybdenum arsenate hydrate ever reported.

Crystal **2** adopts a layer structure, and its polyhedral representations are shown in Figure 4. The basic building unit of a layer is a four-membered ring formed of two pairs of corner-shared MoO_6 octahedra and $HAsO_4$ tetrahedra (Figure 5). Within the layers, large windows of eight-membered rings are generated by connecting four four-membered rings via corner sharing. Similar eight-membered rings of alternating polyhedra exist in $K_{0.17}MoP_2O_7$,[41] $AgMo_5P_8O_{33}$,[42] and $A(MoO_2)(H_2O)(PO_4)$ ($A = K, NH_4$).[39,40] The latter compounds are also layered in which the 8-rings interlink to form polyhedral sheets having the same connectivity as that in **2**. Along the *a*-axis the porous sheets are stacking right on top of each other so that one can see through the 8-ring windows as though there are straight tunnels. Cations and water molecules are residing in the “tunnels”. They provide connections between layers via O−Sr−O bonds and weak H-bonding between the arsenate oxygen and water molecules.

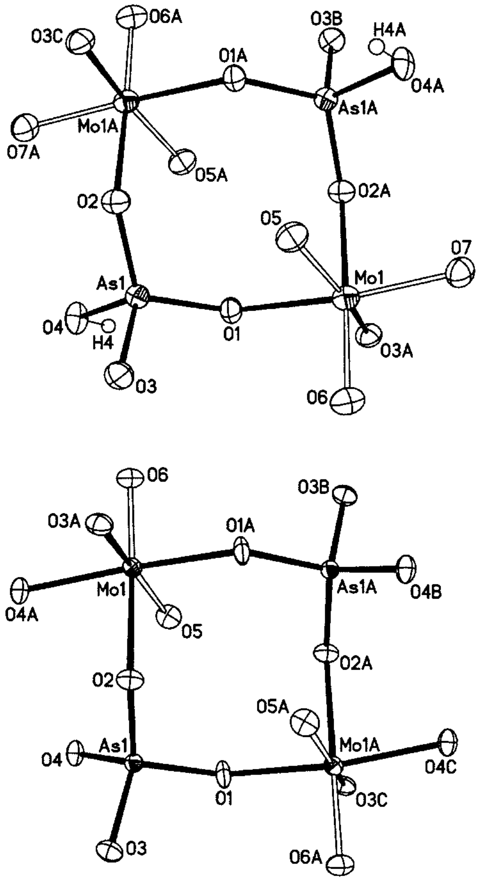

Figure 5. Four-membered rings as basic building units in structure **2** (top) and **3** (bottom). Both sit on inversion centers. Note that MoO_6 octahedra contain facial $\{MoO_3\}$ cores in **2** but cis $\{MoO_2\}$ cores in **3**. Thermal ellipsoids are given at the 50% level.

As in **1**, all of the MoO_6 octahedra contain three terminal O^{2-} ions, and each of the O_{term} atoms receives a nearly equal bond-valence from the Sr^{2+} cations in **2**. In contrast to **1**, however, the three $Mo{=}O_{term}$ bonds in **2** are quite dispersed: two short bonds, 1.716 Å for Mo(1)=O(6) and 1.727 Å for Mo(1)=O(5), and one long bond, 1.848 Å for Mo(1)=O(7). The latter is abnormally long for a terminal Mo=O bond.[31−37] Bond-valence sums for both O(5) and O(6) atoms are well-saturated, but it is only 1.5 vu for O(7), suggesting the facial $\{MoO_3\}$ units are less stabilized in the layered structure of **2**.

---

(35) Schroeder, F. A. *Acta Crystallogr.* **1975**, *B31*, 2294.

(36) Bakakin, V. V.; Klevtsova, R. F.; Gaponenko, L. A. *Kristallografiya* **1982**, *27*, 38.

(37) Hazen, R. M.; Finger, L. W.; Mariathasan, J. W. E. *J. Phys. Chem. Solids* **1985**, *46*, 253.

(38) According to the IR spectrum, the coordinated H_2O is considered to be involved in hydrogen bonding. However, the strength of the H-bonds cannot be properly estimated since the positions of water hydrogen atoms could not be located on difference electron-density maps.

(39) Peascoe, R.; Clearfield, A. *J. Solid State Chem.* **1991**, *95*, 83.

(40) Millini, R.; Carati, A. *J. Solid State Chem.* **1995**, *118*, 153.

(41) Leclaire, A.; Borel, M. M.; Grandin, A.; Raveau, B. *J. Solid State Chem.* **1989**, *78*, 220.

(42) Lii, K. H.; Johnston, D. C.; Goshorn, D. P.; Haushalter, R. C. *J. Solid State Chem.* **1987**, *71*, 131.

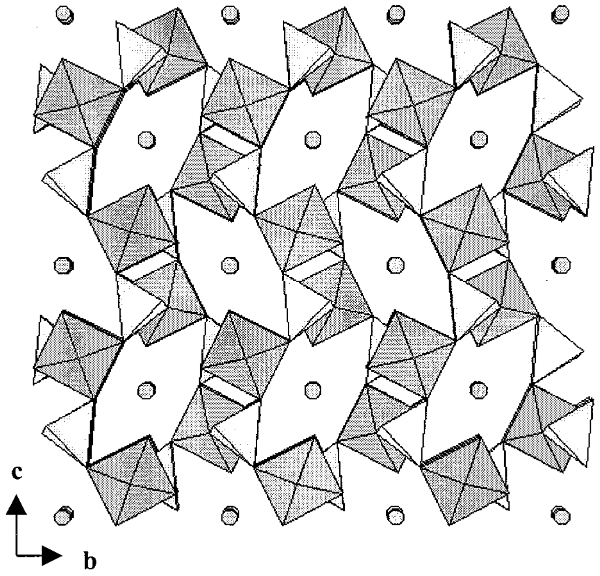

Figure 6. A perspective view of structure **3** along the [100] direction.

Crystals of **3** adopt the same structure as that of the tunneled phosphates $A(MoO_2)_2(PO_4)_2$ (A = Ba, Pb).[43] Polyhedral representation of the structure along [100] and [110] are given in Figures 6 and 7, respectively. It is noted that the building unit in **3** is similar to that in **2** except that the MoO_6 octahedra possess cis $\{MoO_2\}$ cores instead of the facial $\{MoO_3\}$ units (see Figure 5). Each polyhedron in the building unit of **3** has two contacts with others, i.e., via the two bridging atoms, O(3) and O(4), but there is only one contact with others via the only bridging atom O(3) in **2**. A second bridging O atom between Mo and As centers must be provided for structural transformation. As depicted in Figure 7, the layers fuse together by bridging the unsaturated and weakly bonded O(7) atoms in one layer to the As atoms in the adjacent layer. The exothermic peak occurring at ca. 620 °C in the DT curve of **2** may account for the bond formation process as elucidated above.

Summary

We have successfully prepared a novel open-framework material **1**, using divalent inorganic cations as the structure-directing reagent and under more rigorous hydrothermal conditions. Layered material **2** was obtained from mild hydrothermal reactions. Both structures are characterized with the facial $\{MoO_3\}$ "anti-Lipscomb" cores, and they are the first extended structures encapsulating $\{MoO_3\}$ units. Our structural study reveals that these units are tightly bound in the 3D open framework of **1** but rather loosely bound in the layered structure of **2**. During progressive heating, the dehydrated of **2** transformed into **3** in which $\{MoO_3\}$ cores no longer exist. Single crystals of material **3** could be separately obtained by the flux-growth method.

The three compounds represent the first members in the alkaline earth metal/$Mo^{VI}/As^{V}/O$ system. We have obtained the Ba analogue of **3** from hydrothermal reactions.[44] But the existence of either a Sr analogue of **1** or a Ba analogue of **2** is still unknown. It would be interesting to prepare the phosphate analogues containing the facial $\{MoO_3\}$ "anti-Lipscomb" units as well. Investigations along these lines are in progress.

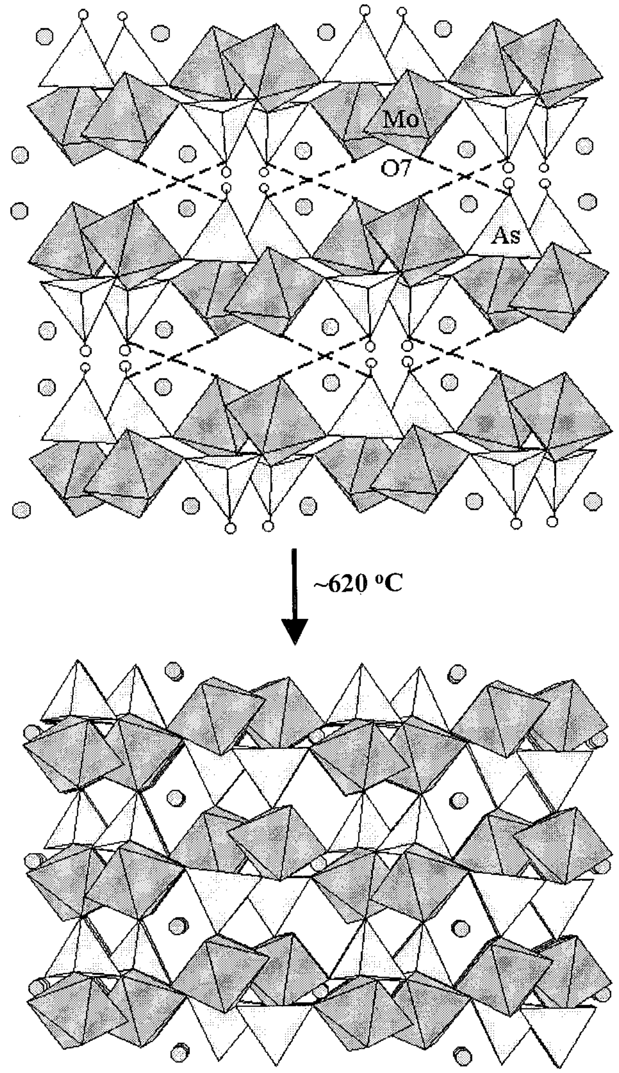

Figure 7. Schematic representation showing structural transformation from **2** to **3**. (top) Projection of structure **2** along the [001] direction. Two layers fuse together by bridging O(7) atoms to As centers in the adjacent layer. (bottom) Projection of structure **3** along the [110] direction.

Acknowledgment. We are grateful to the National Science Council of the Republic of China for support of this work (NSC-88-2113-M007-041).

Supporting Information Available: X-ray crystallographic data including tables of complete crystal data, atomic coordinates, bond distances and angles, and anisotropic thermal parameters for **1**, **2**, and **3**. This material is available free of charge via the Internet at http://pubs.acs.org.

CM990072T

---

(43) Masse, R.; Averbuch-Pouchot, M. T. *J. Solid State Chem.* **1985**, *58*, 157.

(44) A pure phase of colorless tabular crystals of $Ba(MoO_2AsO_4)_2$ can be obtained under a mild hydrothermal condition in which a mixture of $Ba(OH)_2 \cdot 8H_2O$ (0.0789 g, 0.25 mmol), MoO_3 (0.0720 g, 0.50 mmol), 3 M H_3AsO_4 (0.33 mL, 1.0 mmol), and water (0.06 mL, 3.3 mmol) was heated at 250 °C and ~40 atm for 48 h followed by slow cooling (5 °C h^{-1}) to room temperature. Crystal data: monoclinic, $P2_1/c$, $a = 6.5789(4)$ Å, $b = 7.1154(5)$ Å, $c = 10.4004(7)$ Å, $\beta = 93.786(2)°$, $V = 485.80(9)$ Å^3, and $Z = 2$.